

# Compression performance of 3D-printed ant-inspired lattice structures: An innovative design approach

Proc IMechE Part L:  
*J Materials: Design and Applications*  
1–12  
© IMechE 2025  
Article reuse guidelines:  
sagepub.com/journals-permissions  
DOI: 10.1177/14644207241313185  
journals.sagepub.com/home/pil



Mithat Gokhan Atahan<sup>1</sup>  and Selman Saglam

## Abstract

In this study, three different ant-inspired lattice design types: single, double, and inverted double structures were considered due to ants' excellent load-carrying weight ratio. Lattice structures were fabricated using the 3D printing method and polylactic acid filament was used as a printing material. The true blueprint images of the ant were used to obtain the parametric dimensions of the ant-inspired lattice structure. Hence, the presented innovative method for designing lattice structures can be a promising option for industrial sectors requiring high-strength structures. The quasi-static axial compression tests were conducted to evaluate the compression performance of the novel lattice structures. The compression performance of ant-inspired single lattice structures was compared based on specific force, specific energy absorption, and specific stiffness at different height values. The deformation stages and damage regions of ant-inspired lattice structures were analyzed to identify their critical regions during compression tests. The results indicated that as the height value increased, there was a notable decrease in specific force, specific energy absorption, and specific stiffness, along with buckling damage in the ant-inspired single lattice structures. Among the three design types, the ant-inspired inverted double lattice structure showed better compression performance compared to the ant-inspired double lattice structure; however, the ant-inspired single lattice structure with a height of 30 mm exhibited the highest overall compression performance.

## Keywords

Bio-inspired structure, 3D printing, mechanical behavior, lattice structure, additive manufacturing, sustainable manufacturing

Date received: 20 November 2024; accepted: 28 December 2024

## Introduction

Lattice sandwich structures consist of panels and core structures and they are widely used in industrial applications due to their superior properties, including lightweight design, high specific stiffness, high specific strength, and high energy absorption.<sup>1–3</sup> The mechanical properties of lattice structures significantly depend on the design of the core structure; therefore, researchers have sought to enhance these properties through novel core designs.<sup>2–4</sup> Advances in additive manufacturing have enabled the production of novel lattice structures, allowing for the fabrication of lattice structures with excellent energy absorption capabilities for aerospace, automotive, and marine applications.<sup>1,5,6</sup> Ye et al.<sup>7</sup> examined the compression behavior of 3D-printed pyramidal lattice structures. They found that the strength and elastic modulus of the lattice structure increased with increasing slenderness ratio. Uddin et al.<sup>8</sup> improved the compressive properties of 3D-printed pyramidal lattice structures using geometrically tailored I-shaped struts. Han et al.<sup>9</sup> investigated the mechanical properties of novel 3D-printed square auxetic tubular lattice structures.

They reported that novel lattice structures exhibited excellent mechanical properties, making them suitable for engineering applications. Ye et al.<sup>10</sup> conducted axial compressive tests to determine the effects of different printing and structural parameters on the compression performance of 3D-printed X-type lattice structures. They stated that the 3D-printed X-type lattice structure showed superior specific strength, specific stiffness, and energy absorption capability compared to pyramidal lattice structures.

Nature contains unique examples of structures with exceptional mechanical and functional properties.<sup>11</sup> Therefore, bio-inspiration is one of the primary approaches that comes to mind when developing engineering structures.<sup>5</sup> Recently, researchers have focused on developing bio-inspired lattice structures to enhance the

Department of Mechanical Engineering, Abdullah Gül University, Kayseri, Türkiye

### Corresponding author:

Mithat Gokhan Atahan, Department of Mechanical Engineering, Abdullah Gül University, Kayseri, Türkiye. Email: mithatgokhan.atahan@agu.edu.tr

mechanical properties of engineering structures.<sup>12–17</sup> Yin et al.<sup>17</sup> optimized a novel bio-inspired 3D porous structure to enhance its crashworthiness properties. Doodi and Gunji<sup>18</sup> offered novel hybrid bio-inspired 3D-printed lattice structures for aerospace and defense industrial applications. Chouhan et al.<sup>19</sup> examined the mechanical behavior of 3D-printed bio-inspired (centriole, nautilus, and cartwheel) lattice structures. Ramakrishnan et al.<sup>20</sup> proposed the 3D-printed bio-inspired Xylocopa lattice structure for energy absorption applications. Ullah et al.<sup>21</sup> analyzed the mechanical performance of the bio-inspired kagome truss core structures produced using the selective laser melting technique. They found that kagome truss structures exhibited better specific strength than conventional honeycomb structures under compression and shear loads. Doodi et al.<sup>22</sup> investigated the compression behavior of a novel bio-inspired 3D-printed lattice structure. Their design is based on the unit cells derived from the *Papilio xuthus* butterfly species. Du et al.<sup>23</sup> examined the effects of processing parameters on densification behavior, microstructure, and mechanical properties of bio-inspired lattice structures based on the beetle's front wing. The optimized processing parameters resulted in superior energy absorption capability. Sharma and Hiremath<sup>24</sup> proposed novel bio-inspired lattice structures based on *Euplectella Aspergillum* for energy absorption applications.

The ants exhibit excellent load-bearing capabilities due to the intricate balance of forces within their anatomical structure, allowing them to carry loads several times their body weight and navigate challenging terrains despite their small size.<sup>25,26</sup> Therefore, in this study, novel lattice structures inspired by ant anatomy were developed and the effects of height value and design configuration on the compression performance of ant-inspired lattice structures were experimentally investigated. Three different height values (30, 50, and 70 mm) were used to examine the compression performance of the ant-inspired single lattice structures. Ant-inspired single, double, and inverted double lattice design types were developed to determine the effects of the design configurations on the compression performance of the lattice structures. Ant-inspired lattice structures were produced using a 3D printing technique and their compression performance was determined through quasi-static compression tests. The true blueprint images, representing three different views of the ant, were used to create the 3D model in Solidworks design software.<sup>27</sup> Using the ant 3D model, the strut parametric dimensions of the bio-inspired lattice structure were determined. To the best of the authors' knowledge, this study represents the first instance of creating a bio-inspired lattice structure using true blueprint images of an ant.

## Material and method

### Design of lattice structures

An innovative bio-inspired lattice design approach is presented in this study. The schematic representation of the stages of this innovative design approach is presented in Figure 1. First, three different views of the ant's blueprint

images were imported into multiple planes in the Solidworks software, and the Project Curves tool was used to create the 3D-ant model in the Solidworks software (Figure 2(a)). Then, the body surface of the ant was created using the Loft, Sweep, and Boundary Surface commands. Loft surfaces help in smoothly transitioning between different cross-sectional profiles of the body, while Sweep is ideal for the long, slender forms of the legs and antennae. Boundary Surface commands are particularly useful for filling in intricate areas where precise control over the surface shape is required. The parametric distance values between the ant's legs and the angles between the ant's leg and the ground planes were determined using the obtained 3D-ant model (Figures 3 and 4 and Tables 1 and 2). In this way, parametric design parameters were derived from the true anatomical dimensions of the ant and lattice structures were designed using true geometrical parameters. Three different lattice structures, ant-inspired single lattice design (Figure 5(a)), ant-inspired double lattice design (Figure 5(b)), and ant-inspired inverted double lattice design (Figure 5(c)), were considered to investigate the effect of the different height values and design configuration on the compression performance of ant-inspired lattice structures. The effect of height values on the compressive performance of ant-inspired lattice structures was investigated using ant-inspired single lattice structures with different strut height values of 30, 50, and 70 mm (Figure 2(b)). The effect of the design configuration on the compressive behavior of lattice structures was evaluated using the ant-inspired double lattice design and the ant-inspired inverted double lattice design, both with the same height value (Figures 5(b) and (c)). The double and inverted double ant-inspired lattice structures were created by mirroring the single lattice design in Solidworks. The strut diameter is 6 mm for all lattice design types.<sup>7</sup> The distance parameters between the struts are represented by A, B, C, D and E, and the parametric distance ratio values of the struts are presented in Table 1. The K value, which represents the parametric ratio, was selected as 1 in this study. The angle values between the struts and axes, which play a critical role in the structural integrity and load capabilities of the designs, are illustrated in Table 2. The angle parameters between the struts and axes in the 3D-plane are shown schematically in Figure 4. The angle values between the struts and axes were obtained directly from the 3D-ant model. Furthermore, each structure has a unique panel size due to variations in height, while maintaining consistent strut angles across all designs. The panel length values of the lattice structures are presented in Table 3 and Figure 4. The thickness value of each panel was selected as 3 mm.

### Manufacturing process of the lattice structures

Lattice structures were produced using the fused deposition modeling (FDM) method. After lattice designs were obtained using an innovative design approach,

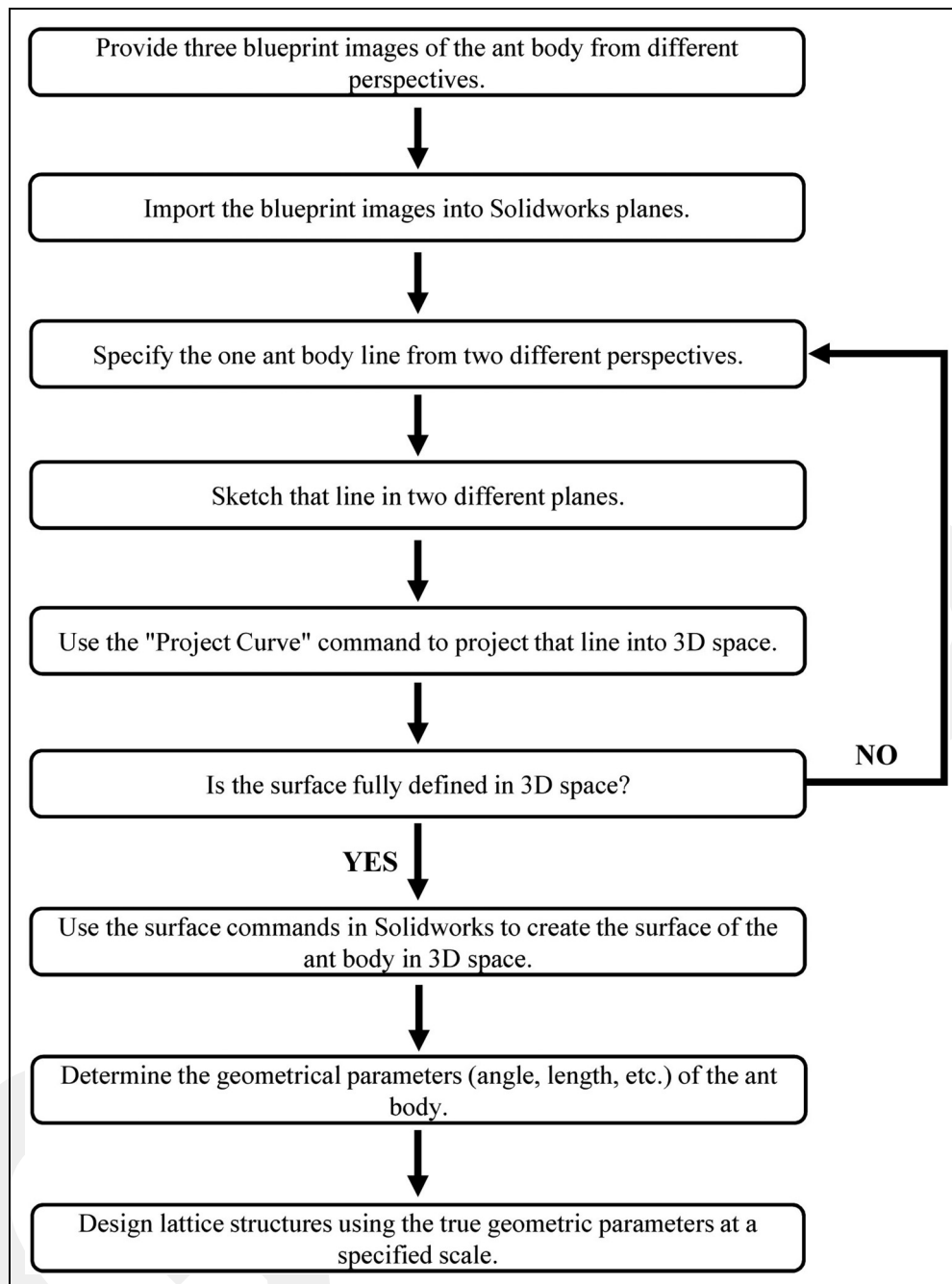


**Figure 1.** Flowchart of the innovative ant-inspired lattice design approach stages.

they were converted to STL (Stereolithography) files using Solidworks design software. G-codes (printing codes) were generated from the STL files using Ultimaker Cura software.<sup>28</sup> The filaments were laid parallel to the loading direction to minimize bending damage (Figure 2(c)). Ant-inspired lattice structures were produced using an Ultimaker 3 3D printer (Figure 2(d)). Polylactic acid (PLA) was chosen as the 3D printing material. PLA is a kind of biodegradable thermoplastic polymer widely used in additive manufacturing method.<sup>29,30</sup> It is produced from renewable resources like tapioca roots, corn starch or sugar cane.<sup>30</sup> Moreover, printed parts produced from PLA can be recycled. Therefore, lattice structures produced from

PLA offer sustainable manufacturing. The printing and build plate temperatures were set to 210 °C and 60 °C, respectively. The printing speed was chosen as 50 mm/min. All lattice structures were fabricated with 100% infill density, and the shell wall thickness was set to 0.5 mm. PLA filament with a diameter of 2.85 mm was used to manufacture the lattice structures. The layer height was set to 0.1 mm with a nozzle diameter of 0.4 mm. The lattice structures were printed without support. Printed ant-inspired lattice structures were weighed using a precision electronic balance to determine their specific compression performance parameters, and the measured weight values of the sandwich core designs are listed in Table 4.

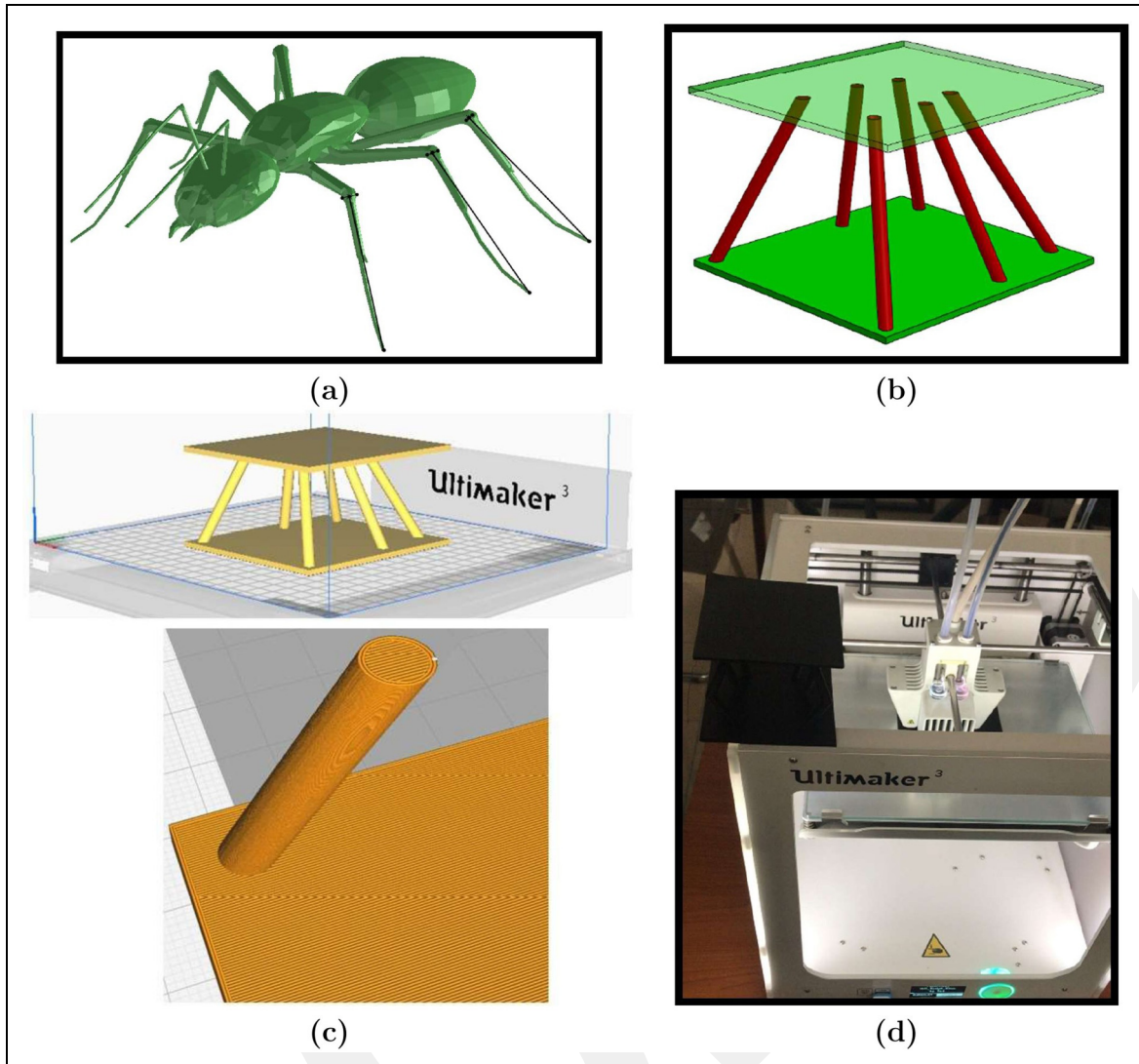


**Figure 2.** Demonstration of (a) obtaining the 3D model of the ant, (b) 3D design of the ant-inspired single lattice structure, (c) filament raster orientation, and (d) manufacturing of the ant-inspired lattice structure.

### Compression test

Compression tests were conducted using a Shimadzu universal testing machine at a constant loading speed of 2 mm/min. The machine has a high-precision load cell with a load-carrying capacity of 10 kN. Compression tests of the lattice structures were recorded with a digital camera to observe the progressive deformation and damage mechanisms. Three repeated tests were performed for each design type to verify the test results. A compressive load was applied to the lattice structures until failure occurred. Force-displacement curves for the lattice structures were obtained after the compression tests. The test machine has a computer control and data acquisition system, allowing both force and displacement data to be automatically obtained. Compression performance indicators, such as maximum load-carrying capacity, absorbed energy, and stiffness parameters, were determined from the obtained force-displacement curves of the lattice structures. The maximum load-carrying capacity of the lattice structures was determined using the highest force value from the force-displacement curve. The area under the force-displacement

curve was determined using a MATLAB script with the Trapezoidal Method. This area represents the amount of energy absorbed by the lattice structures under compressive load. The stiffness of the lattice structures is related to their damage-tolerant performance. The stiffness values of the lattice structures were calculated from the slope of the elastic loading line in the force-displacement curve (tangent modulus). Two points were selected on the elastic loading curve (linear curve), and the slope of the line was determined using these points. This slope value indicates the stiffness of the lattice structure. Compression test results were normalized using the weight values of the lattice structures to compare their compression performances.

## Results and discussion

### Ant-inspired single lattice structures

The buckling sensitivity and damage mechanisms of the lattice structures are influenced by changes in height.<sup>7</sup>

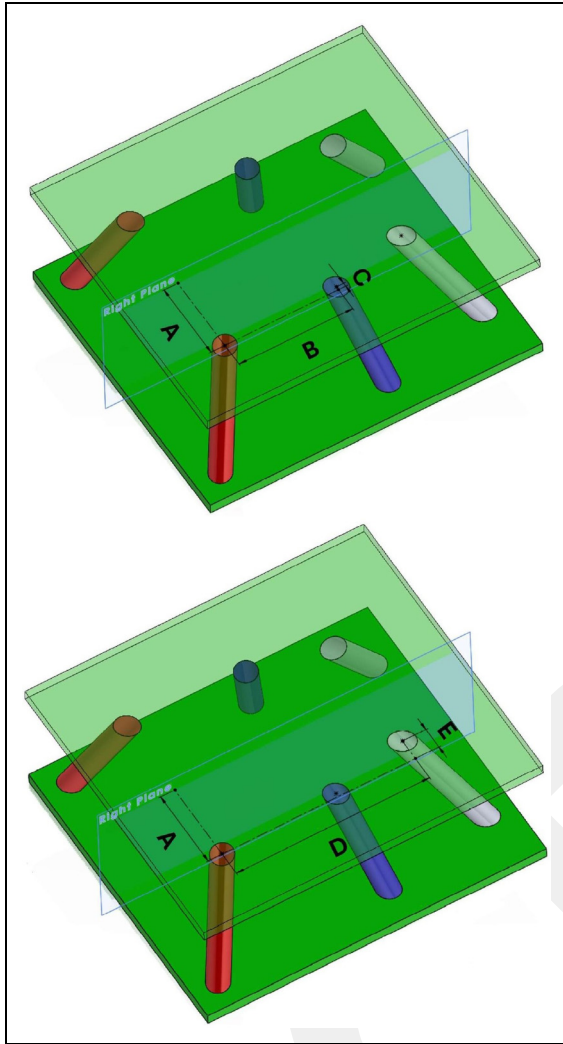


**Figure 3.** Illustration of parametric dimensions of the struts.

Therefore, the effects of different lattice height values on the load-carrying capacity, energy absorption, and stiffness of novel ant-inspired single lattice structures were investigated comprehensively.

**Specific force.** The load-carrying capacity of lattice structures is crucial for industrial applications. In engineering applications, lattice structures with varying height values are often desired, making it crucial to determine the impact of height on their load-carrying capacity for the design of high-strength structures. The load-carrying capacities of ant-inspired single lattice structures with different height values are presented in Figure 6(a). The load-carrying capacities of the lattice structures were determined based on the maximum force value recorded during the compression test. The maximum force values of the lattice structures were normalized using their weight values. The lattice structure with a height of 30 mm exhibited the highest load-carrying capacity. As the height value of the lattice structures increased, the load-carrying capacity decreased significantly. Namely, when the height of the lattice structures increased from 30 mm to 50 mm, the load-carrying capacity decreased by

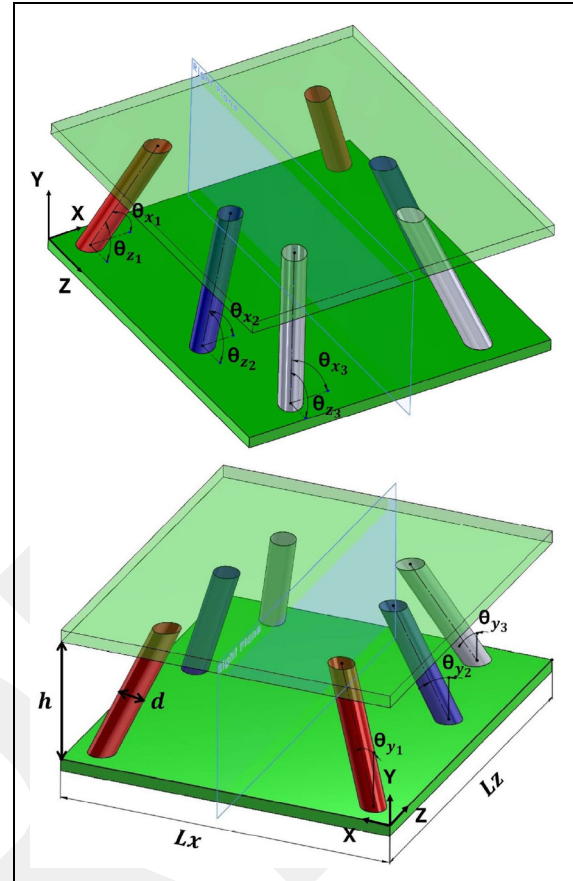


**Figure 4.** Demonstration of angle parameters between the struts and axes.

**Table I.** Parametric distance ratio values of the struts.

Ratio	A (mm)	B (mm)	C (mm)	D (mm)	E (mm)
K=1	21.80 K	31.65 K	1 K	52.65 K	6K

approximately 2 times; further increasing the height to 70 mm resulted in a reduction of about 6 times. It was found that the height of the lattice structures significantly affected their load-carrying capacity. As the height of the lattice structures increased, their buckling sensitivity also increased, leading to strut buckling deformation rather than stable vertical deformation under compressive load. Strut buckling deformation deteriorated the stability of the lattice structures, leading to premature failure and a significant reduction in their load-carrying capacity. While single lattice structures can withstand a compression load of 2560–6300 N, double lattice structures can carry a compression load of 250–480 N. Compared to the load-carrying capacities of lattice structures, panel weights (22.80–61.70 g) are negligible. In this study, the load-carrying capacities of lattice structures were determined by neglecting the panel weights.

**Specific energy absorption.** Figure 6(b) depicts the specific energy absorption values of ant-inspired single lattice structures with different height values. The specific energy

absorption values of the lattice structures were calculated by dividing the area under the force-displacement curve by the weight of the structures. Lattice structures are sought for their high energy absorption capabilities in industrial applications. Compared to lattice structures with heights of 50 mm and 70 mm, the lattice structure with a height of 30 mm exhibited the highest energy absorption capability, absorbing approximately 2.5 times more energy than the 50 mm structure and 6 times more than the 70 mm structure. Strut buckling damage reduced the vertical deformation capacity of the lattice structures, consequently decreasing their energy absorption ability.

**Specific stiffness.** The stiffness of the lattice structure was calculated using the slope of the loading line on the force-displacement curve and was normalized by

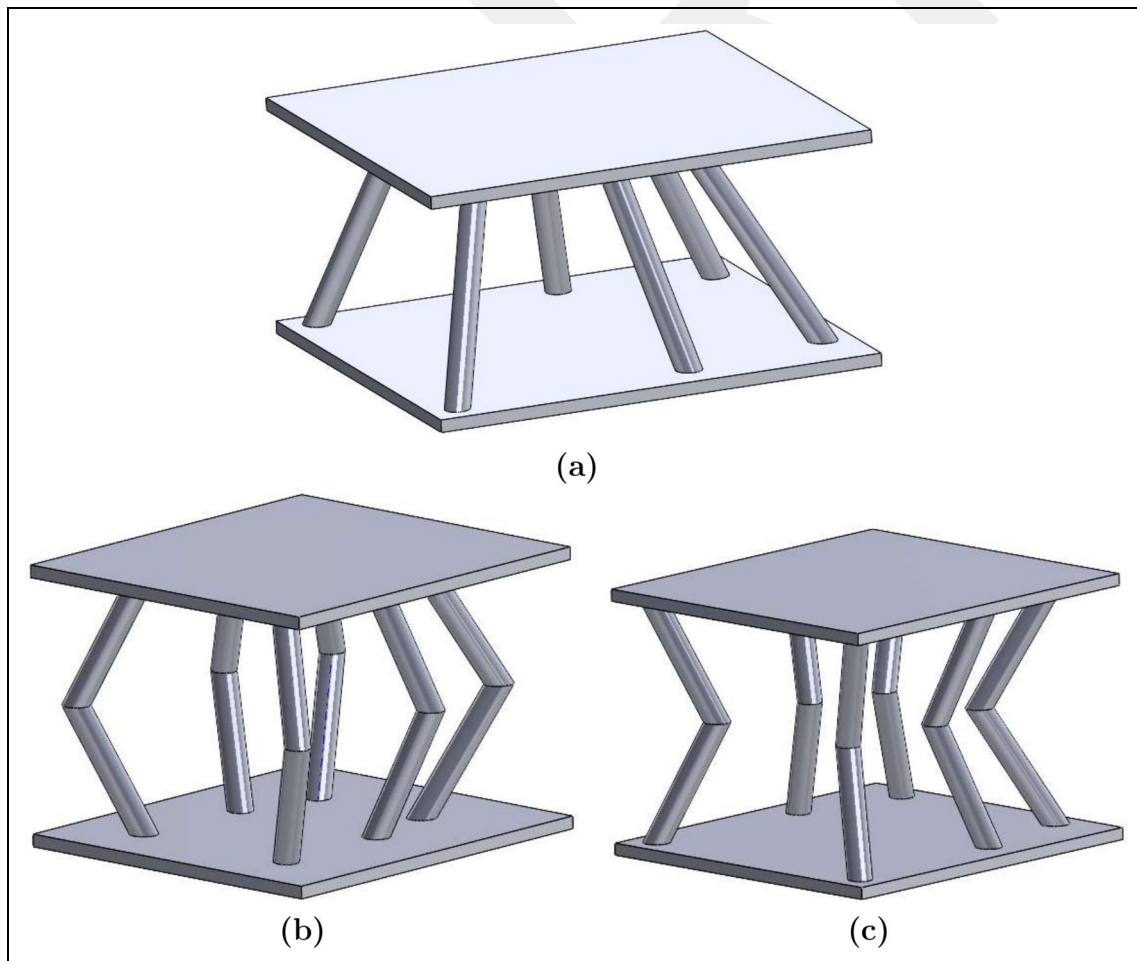
**Table 2.** Angle values between struts and axes (x, y, and z).

Axes Name	Red Strut	Blue Strut	Grey Strut
$\theta_x$	111.15°	109.55°	106°
$\theta_y$	26.85°	23.30°	31.90°
$\theta_z$	74.20°	102.25°	116.85°

the weight of the structure. The specific stiffness values of ant-inspired single lattice structures with varying height values is illustrated in Figure 6(c). The stiffness values of lattice structures offer insight into their damage-tolerant performance.<sup>4,31</sup> An increase in stiffness improves the damage-tolerant performance of the lattice structure. The lattice structure with a height of 30 mm exhibited the highest specific stiffness value. As the height of the lattice structures increased, the specific stiffness values decreased significantly. Namely, increasing the height of the lattice structure reduced its damage-tolerant performance. The lattice structure with a height of 70 mm showed the lowest damage-tolerant performance. The

**Table 3.** Panel length values of the lattice structures.

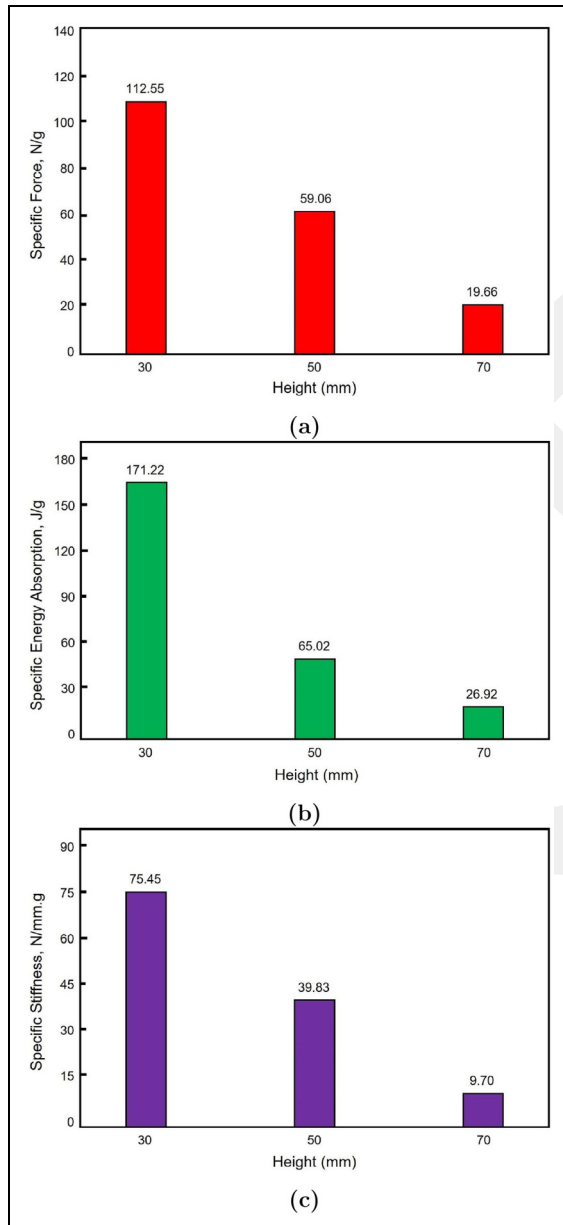
Design Configuration	Height (mm)	$L_x$ (mm)	$L_z$ (mm)
Single	30	82.30	92.25
	50	98.50	109
	70	122.70	134.10
Double Inverted double	50	82.30	92.30
	50	82.30	92.30



**Figure 5.** Lattice design types: (a) ant-inspired single lattice design, (b) ant-inspired double lattice design and (c) ant-inspired inverted double lattice design.

**Table 4.** Weight values of ant-inspired lattice structures.

Design Configuration	Height (mm)	Weight (g)
Ant-inspired single lattice structure	30	56.01
	50	74.61
	70	130.35
Ant-inspired double lattice structure	50	55.21
Ant-inspired inverted double lattice structure	50	65

**Figure 6.** Comparison of (a) specific force, (b) specific energy absorption, and (c) specific stiffness variations according to the different height values of ant-inspired single lattice structures.

increase in height of the lattice structure led to strut buckling deformation, which deteriorated its damage-tolerant performance.

### Effect of the design configurations

In this study, two lattice design configurations, double and inverted double, were considered to examine the effects of design configurations on compression performance. Their compression performances were compared based on specific force, specific energy absorption, and specific stiffness parameters (Figure 7). The load-carrying capacity of the inverted double lattice structure was approximately 1.65 times greater than that of the double lattice structure. Moreover, the inverted double lattice structure absorbed approximately 2.1 times more energy than the double lattice structure. The concave design approach enhanced both the load-carrying capacity and the energy absorption capability of the lattice structure. However, the specific stiffness values of both lattice structures were similar. While the increase in the height of the lattice structure significantly affected its damage-tolerant performance, the different design configurations had little effect on this performance. Additionally, the single lattice structure with a height of 50 mm demonstrated better compression performance than both the double and inverted double structures.

### Progressive damage analysis

The deformation mechanism and damage analysis of single, double, and inverted double lattice structures under compressive load were comprehensively investigated. Figure 8 illustrates the deformation stages and damage regions of ant-inspired single lattice structures with varying height values. Red circles indicate damaged regions in the lattice structures. The single lattice structure with a height of 70 mm exhibited the highest deformation capability compared to the other structures. Increasing the height of the lattice structure enhanced its deformation capability. While balanced collapse deformation was observed in the single lattice structure with a height of 30 mm, unbalanced vertical deformation occurred in the single lattice structures with heights of 50 and 70 mm due to strut buckling damage. Increasing the height of the lattice structures decreased the buckling stiffness of the struts and early damage development was observed in some struts. The vertical compressive force applied to lattice structures has two components: an axial force along the direction of the strut's cross-section and a tangential force perpendicular to the strut's cross-section.<sup>7</sup> The axial force causes buckling of the struts, while the tangential force induces shear force and bending moment in the cross-section. Progressive damage analysis enables the evaluation of loading conditions that influence the deformation mechanism of the struts. In the progressive damage analysis of single lattice structures, it was observed that the struts predominantly underwent lateral deformation. Therefore, it was determined that the buckling load was more effective in the damage mechanism of single lattice structures.

The deformation stages and damage regions of the ant-inspired double and inverted double lattice structures

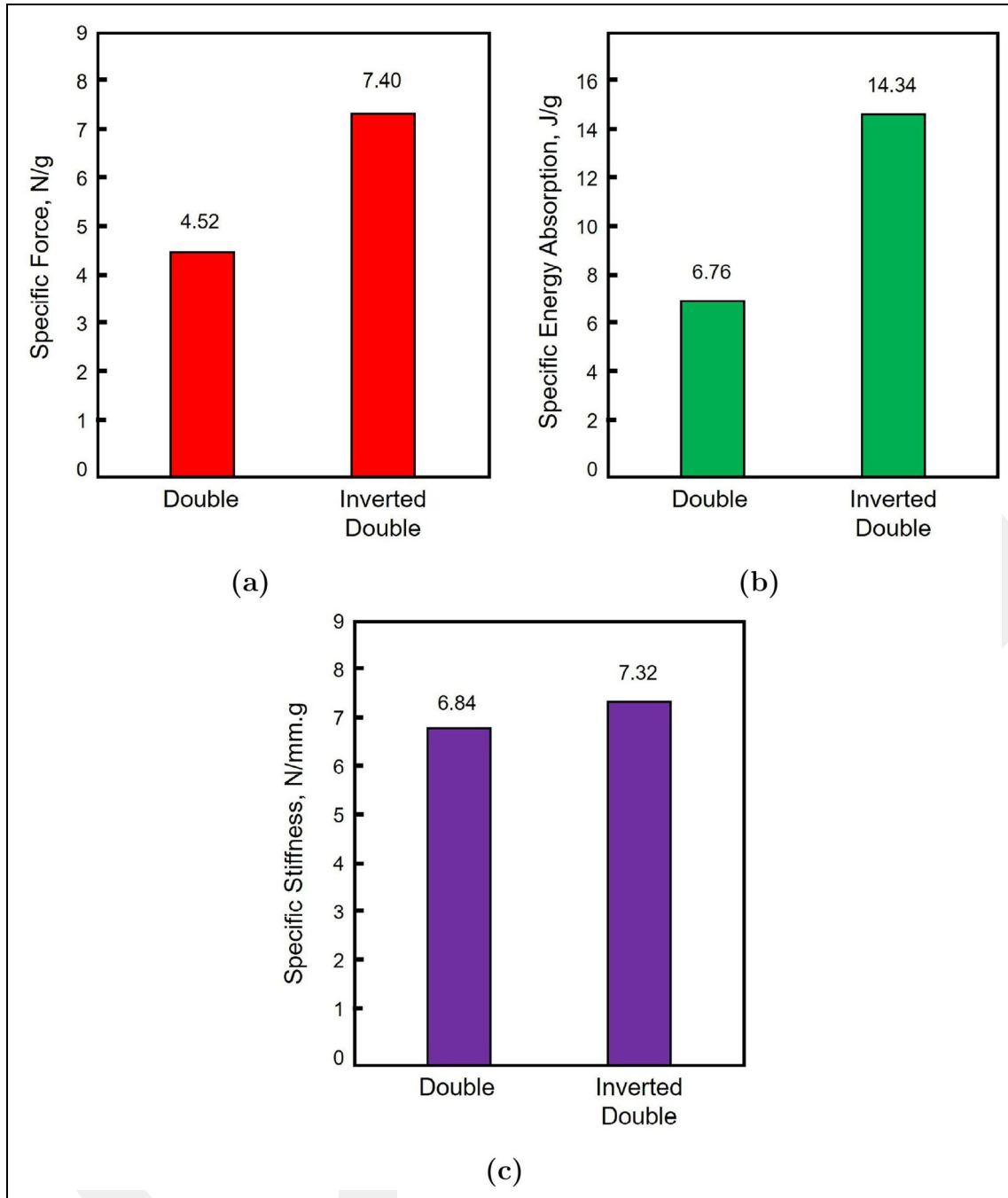


**Figure 7.** Comparison of (a) specific force, (b) specific energy absorption, and (c) specific stiffness variations of the ant-inspired double and inverted double lattice structures.

are illustrated in Figure 9. A gradual damage mechanism was observed in both lattice structures. Therefore, it caused fluctuations in the force-displacement curves of the double and inverted double lattice structures. The inverted double structure had greater deformation capability. The concave structure (inverted double) showed greater load-carrying capacity and damage-tolerant performance. While the damage in the double lattice structure occurred in the connected regions of two struts, in the inverse double lattice structure, damage was observed both in the connected regions of the two struts and in the regions between the struts and the panel. PLA has high deformation

capability. The lattice structure experienced panel deformation during initial loading. Then, the struts became effective in carrying the compressive load. Therefore, at the initial loading stage, the force-displacement curve increased with a low slope. The slope of the loading curve increased as the struts also carried the compression load, and the slope of this curve represents the stiffness of the lattice structure. As plastic deformation began, the force-displacement curve exhibited non-linear characteristics. When the lattice structure reached its maximum load-carrying capacity, complete failure occurred, and the force-displacement curve dropped sharply.

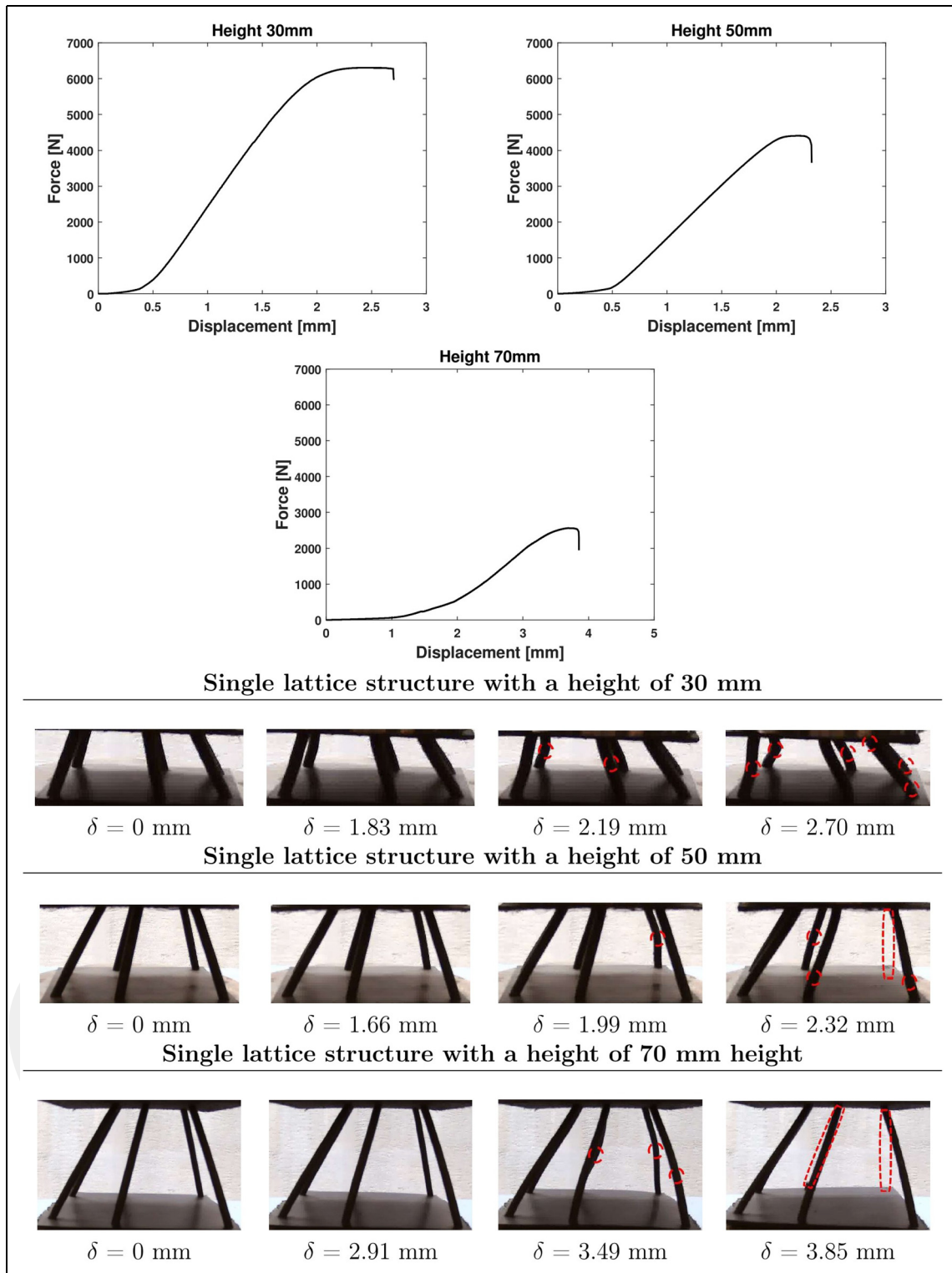


**Figure 8.** Deformation stages and damage regions of ant-inspired single lattice structures with varying height values.

It is worth mentioning that the deformation and damage mechanisms of the lattice structures depend on the selected filament raster orientation, the filament material used, and the preferred additive manufacturing method.<sup>7</sup> Therefore, the deformation and energy absorption capabilities of lattice structures can be enhanced by selecting different filament raster orientation angles, filament materials, and additive manufacturing methods.

### Conclusions

In this study, an innovative lattice design approach was proposed, and the effects of lattice height values and design configurations on the compression performance of the lattice structures were investigated comprehensively. The main conclusions of this research were listed as follows:

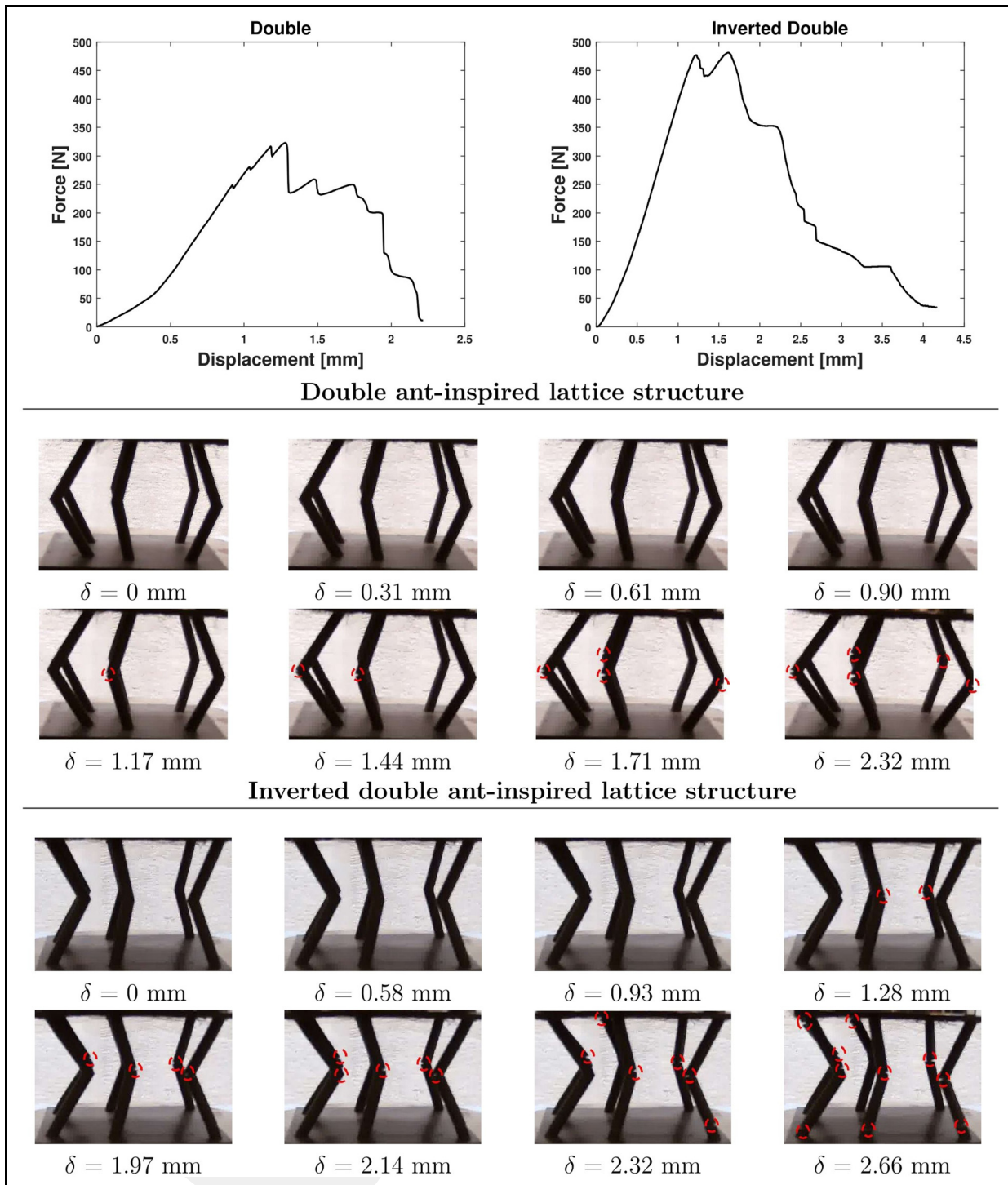


**Figure 9.** Deformation stages and damage regions of ant-inspired double and inverted double lattice structures.

- Thanks to the innovative design approach, lattice structures were designed with true geometrical parameters of the bio-inspired structure.
- The increase in the height of single lattice structures negatively affected their compression performance. As the height of the single lattice structures increased from 30 mm to 50 mm, their load-carrying capacity was reduced by about half. Increasing the height further to 70 mm led to a decrease of approximately six times.
- The increase in the height of single lattice structures heightened the tendency of struts to undergo buckling deformation, leading to premature damage.
- The inverted double lattice structure demonstrated better compression performance compared to the double lattice structure due to its concave strut design. The load-carrying capacity of the inverted double lattice structure was about 1.65 times higher than that of the double lattice structure. Additionally, the inverted double lattice structure absorbed nearly

2.1 times more energy compared to the double lattice structure.

### Acknowledgments

The authors acknowledge the Scientific and Technological Research Council of Türkiye for its financial support (TÜBİTAK-2209A, Project no: 1919B012217484).

### Data availability

Data will be made available on request.

### Declaration of conflicting interests

The authors declared no potential conflicts of interest with respect to the research, authorship, and/or publication of this article.

### Funding

This study was financially supported by the Scientific and Technological Research Council of Türkiye for its financial support (TÜBİTAK-2209A, Project no: 1919B012217484).

### ORCID iD

Mithat Gokhan Atahan  <https://orcid.org/0000-0002-8180-5876>

### References

1. Yin H, Zhang W, Zhu L, et al. Review on lattice structures for energy absorption properties. *Compos Struct* 2023; 304: 116397.
2. Ye G, Bi H, Li Z, et al. Compression performances and failure modes of 3d printed pyramidal lattice truss composite structures. *Compos Commun* 2021; 24: 100615.
3. Zheng T, Li S, Wang G, et al. Mechanical and energy absorption properties of the composite xx-type lattice sandwich structure. *Eur J of Mech- A/Solids* 2022; 91: 104410.
4. Atahan MG, Erikli M, Ozipek E, et al. Comparative study on bending behavior and damage analysis of 3d-printed sandwich core designs with bio-inspired reinforcements. *Eng Fail Anal* 2024; 163: 108439.
5. Ramakrishna D and Bala Murali G. Bio-inspired 3d-printed lattice structures for energy absorption applications: a review. *Proce of the Instit of Mech Eng, L: J of Mater: Des Appl* 2023; 237: 503–542.
6. Palomba G, Epasto G and Crupi V. Lightweight sandwich structures for marine applications: a review. *Mech Adv Mater Struct* 2022; 29: 4839–4864.
7. Ye G, Bi H and Hu Y. Compression behaviors of 3d printed pyramidal lattice truss composite structures. *Compos Struct* 2020; 233: 111706.
8. Uddin MA, Barsoum I, Kumar S, et al. Enhancing compressive performance in 3d printed pyramidal lattice structures with geometrically tailored i-shaped struts. *Mater Des* 2024; 237: 112524.
9. Han D, Ren X, Luo C, et al. Experimental and computational investigations of novel 3d printed square tubular lattice metamaterials with negative poisson's ratio. *Addit Manuf* 2022; 55: 102789.
10. Ye G, Bi H, Chen B, et al. The compression performance of 3d-printed x structures. *Mater Des* 2022; 224: 111380.
11. San Ha N and Lu G. A review of recent research on bio-inspired structures and materials for energy absorption applications. *Compos B Eng* 2020; 181: 107496.
12. Wang M, Zhang J, Wang W, et al. Compression behaviors of the bio-inspired hierarchical lattice structure with improved mechanical properties and energy absorption capacity. *J Mater Res Technol* 2022; 17: 2755–2771.
13. Tan C, Zou J, Li S, et al. Additive manufacturing of bio-inspired multi-scale hierarchically strengthened lattice structures. *Int J Mach Tools Manuf* 2021; 167: 103764.
14. Huang Z, Li B, Ma L, et al. Mechanical properties and energy absorption performance of bio-inspired dual architecture phase lattice structures. *Mech Adv Mater Struct* 2023; 30: 1842–1852.
15. Li B, Liu H, Zhang Q, et al. Crushing behavior and energy absorption of a bio-inspired bi-directional corrugated lattice under quasi-static compression load. *Compos Struct* 2022; 286: 115315.
16. Sharma D and Hiremath SS. Experimental and fem study on the in-plane and out-plane loaded reversible dual-material bio-inspired lattice structures with improved energy absorption performance. *Compos Struct* 2023; 303: 116353.
17. Yin H, Zheng X, Wen G, et al. Design optimization of a novel bio-inspired 3d porous structure for crashworthiness. *Compos Struct* 2021; 255: 112897.
18. Doodi R and Gunji BM. An experimental and numerical investigation on the performance of novel hybrid bio-inspired 3d printed lattice structures for stiffness and energy absorption applications. *Mech Adv Mater Struct* 2023; 31: 3970–3979.
19. Chouhan G, Gunji BM, Bidare P, et al. Experimental and numerical investigation of 3d printed bio-inspired lattice structures for mechanical behaviour under quasi static loading conditions. *Mater Today Commun* 2023; 35: 105658.
20. Ramakrishnan R, Hemanth Kumar J, Titus F, et al. Experimental investigation of 3d printed bio-inspired xylofus lattice structure for energy absorption under quasi-static axial loading conditions. *Proce of the Instit of Mech Eng, L: J of Mater: Des Appl* 2024; 238: 1942–1955.
21. Ullah I, Elambasseril J, Brandt M, et al. Performance of bio-inspired kagome truss core structures under compression and shear loading. *Compos Struct* 2014; 118: 294–302.
22. Doodi R, Gunji BM and Raju bahubalendruni M. Compression behavior of bio-inspired lattice structures inspired by papilio Xuthus. *Mater Today Proc* 2023; 90: 184–187.
23. Du Y, Gu D, Xi L, et al. Laser additive manufacturing of bio-inspired lattice structure: forming quality, microstructure and energy absorption behavior. *Mater Sci Eng A* 2020; 773: 138857.
24. Sharma D and Hiremath SS. Bio-inspired repeatable lattice structures for energy absorption: experimental and finite element study. *Compos Struct* 2022; 283: 115102.
25. Merienne H, Latil G, Moretto P, et al. Dynamics of locomotion in the seed harvesting ant messor barbarus: effect of individual body mass and transported load mass. *PeerJ* 2021; 9: e10664.
26. Bernadou A, Felden A, Moreau M, et al. Ergonomics of load transport in the seed harvesting ant messor barbarus: morphology influences transportation method and efficiency. *J Exp Biol* 2016; 219: 2920–2927.
27. *SOLIDWORKS™ 3D Design Software - Dassault Systèmes*. Available from: <https://www.3ds.com/products-services/solidworks/?wockw=Solidworks>.

28. Ultimaker Cura: Powerful, easy-to-use 3D printing software. Available from: <https://ultimaker.com/software/ultimaker-cura>.
29. Azzouz L, Chen Y, Zarrelli M, et al. Mechanical properties of 3-d printed truss-like lattice biopolymer non-stochastic structures for sandwich panels with natural fibre composite skins. *Compos Struct* 2019; 213: 220–230.
30. Tunay M. Bending behavior of 3d printed sandwich structures with different core geometries and thermal aging durations. *Thin-Walled Struct* 2024; 194: 111329.
31. Liu Z, Chen H and Xing S. Mechanical performances of metal-polymer sandwich structures with 3d-printed lattice cores subjected to bending load. *Arch of Civil and Mech Eng* 2020; 20: 89.

GCRIIS